

1 **Ion exchange resins as catalysts for the liquid-phase dehydration of 1-butanol to**
2 **di-n-butyl ether**

3 **M.A. Pérez, R. Bringué, M. Iborra, J. Tejero*, F. Cunill**

4 Department of Chemical Engineering, University of Barcelona, C/Martí i Franquès, 1, 08028 –
5 Barcelona

6 *Corresponding author: Phone: +34 93 402 1308; fax: +34 93 402 1291. E-mail address:

7 jtejero@ub.edu (J. Tejero)

8
9 **Abstract**

10 This work reports the production of di-n-butyl ether (DNBE) by means of 1-butanol dehydration
11 in the liquid phase on acidic ion-exchange resins. Dehydration experiments were performed at
12 150 °C and 40 bar on 13 styrene-codivinylbenzene ion exchangers of different morphology. By
13 comparing 1-butanol conversions to DNBE and initial reaction rates it is concluded that
14 oversulfonated resins are the most active catalysts for 1-butanol dehydration reaction whereas
15 gel-type resins that swell significantly in the reaction medium as well as the macroreticular
16 thermostable resin Amberlyst-70 are the most selective to DNBE. The highest DNBE yield was
17 achieved on Amberlyst 36. The influence of typical 1-butanol impurities on the dehydration
18 reaction were also investigated showing that the presence of 2-methyl-1-propanol (isobutanol)
19 enhance the formation of branched ethers such as 1-(1-methylpropoxy) butane and 1-(2-
20 methylpropoxy) butane, whereas the presence of ethanol and acetone gives place to ethyl butyl
21 ether and, in much lesser extent, diethyl ether.

22 **Keywords:** Di-n-butyl ether (DNBE), ion-exchange resins, 1-butanol dehydration.

23 **1. Introduction**

24 Dependence on fossil fuels has raised two main concerns: on one hand, the associated
25 environmental effects; on the other, oil reserves limitation and future depletion. Given the
26 severity of these threats the European Union has ruled increasingly stringent specifications for:

27 (1) quality of petrol, diesel and gas-oil (Directive 2009/30/EC); (2) emissions from light
28 passenger and commercial vehicles (Regulation EC 715/2007); and (3) promotion of the use of
29 energy from renewable sources, setting a mandatory 10 % minimum target to be achieved by all
30 Member States for the share of biofuels in transport petrol and diesel consumption by 2020
31 (Directive 2009/28/EC).

32 Although very efficient, diesel engines have had difficulties achieving desirable emission
33 targets, especially for soot and NO_x formation [1]. Reformulation of diesel fuel to include
34 oxygenates has proven to be an effective way to provide satisfactory engine power and cleaner
35 exhaust without modification of existing diesel engines [2-5].

36 A number of oxygenates have been considered as components for diesel fuel including various
37 alcohols, ethers and esters. Alcohols have several drawbacks: high water solubility, which can
38 cause phase separation problems; high Reid vapor pressure (RVP), which may lead to the
39 plugging of the fuel flow by increasing the vapor pressure; high volatility, which increases the
40 volatile organic compounds emissions; high latent heat of vaporization, which raises cold start-
41 up and drivability issues; and low heating value [6]. Vegetable oil methyl esters have a number
42 of properties non suitable for diesel fuels such as higher boiling point, viscosity, and surface
43 tension that may contribute to increase the NO_x emissions [7]. On the other hand, ethers show
44 the best properties for diesel blends such as high cetane number, cold flow properties and
45 mixture stability. In a comprehensive study on the blending properties of different oxygenates in
46 diesel fuel, including monoethers, polyethers and esters, it was observed that linear monoethers
47 with more than 9 carbon atoms showed the best balance among blending cetane number and
48 cold flow properties which are measured by the Cloud Point (CP) and the Cold Filter Plugging
49 Point (CFPP) [8]. Linear ethers have also shown to be effective in reducing diesel exhausts such
50 as CO, particulate matter and unburned hydrocarbons and to substantially improve the trade-off
51 between particulate and NO_x due to the presence of oxygen in the ether molecules [9].

52 It is quoted in the open literature that linear symmetrical ethers are produced by bimolecular
53 dehydration of primary alcohols over acid catalysts [10],[11]. Nowadays the main synthesis

54 route of primary alcohols is based on the oxo process. It consists of selective hydroformylation
55 and hydrogenation of linear olefins from fluid catalytic cracking in the presence of Rh and Co
56 phosphines [12]. In this way 1-butanol is mainly produced by the oxo synthesis process of
57 propylene in which aldehydes from propylene hydroformylation are hydrogenated to yield 1-
58 butanol. With this hydrogenation step 1-butanol is obtained jointly with 2-methyl-1-propanol
59 (isobutanol) as byproduct. Afterwards, the bimolecular dehydration reaction of the primary
60 alcohol gives the corresponding ether. Although superior alcohols can also be produced from
61 biomass by condensation of bioethanol and/or biomethanol (Guerbet Catalysis) [13], this is still
62 a developing technology which is not yet commercialized [14]. However, biomass fermentation
63 by microorganisms of the genus *Clostridium* giving place to 1-butanol along with acetone and
64 ethanol (Acetone Butanol Ethanol or ABE fermentation) is being performed on the industrial
65 scale [15], [16]. Thus, di-n-butyl ether can be considered a promising oxygenate to blend with
66 diesel fuel as it keeps a good balance between cetane number and cold flow properties [17] and,
67 in addition, it can be obtained from biomass and therefore, it could compute for the biofuel
68 target.

69 Both an intermolecular dehydration (ether formation) and an intramolecular dehydration (olefin
70 formation) may occur in the alcohol dehydration reaction. The prevailing pathway depends on
71 the reaction conditions as well as the reactant and catalyst used. Solid acids such as zeolites
72 [18], aluminum phosphates [19], amorphous aluminosilicates (AAS) [18], microporous niobium
73 silicates [20], η -alumina [17], and heteropolyacids [21],[22] have been tested as catalysts in the
74 dehydration of 1-butanol. In the gas phase selectivity is highly dependent on conversion. Over
75 AlPO_4 the dehydration of 1-butanol gives place mainly to butenes at 1-butanol conversions >75
76 % (fixed-bed reactor, atmospheric pressure, $T= 300^\circ\text{C}$), what suggests that the intramolecular
77 dehydration of 1-butanol to 1-butene and the subsequent isomerization to trans-2-butene and
78 cis-2-butene take place [19]. Butene was the major product for the dehydration reaction on AAS
79 over the whole temperature tested (flow microreactor, 105 – 185 °C, 1 atm) [18]. At the same
80 set-up and experimental conditions, selectivity to ether over H-ZSM-5 was higher than on AAS

81 at about 2% alcohol conversion, but it decreased remarkably on increasing 1-butanol conversion
82 [18]. In the dehydration of C₅ – C₁₂ linear alcohols over η- alumina (fixed bed reactor, 250 –
83 350 °C, 0 – 4 MPa, WHSV = 1 – 4 h⁻¹) it was observed that temperatures as high as 300 °C were
84 necessary to achieve over 60 % conversion of 1-butanol; selectivity to ethers being lower than
85 30% [17]. Finally, 1-butanol dehydrated selectively to butenes over microporous niobium
86 silicate as well (150 – 300 °C, 1 atm) [20]. On the contrary, the liquid phase etherification of 1-
87 butanol to di-n-butyl ether has been studied on heteropolyacids with different heteroatoms (200
88 °C, 30 bars) showing that 1-butanol dehydrates selectively to di-n-butyl ether achieving over
89 80% ether selectivity with 1-butanol conversions ranging from 30 to 80% [22].

90 It is well-known fact that acidic ion-exchange resins are highly selective catalysts to produce
91 linear symmetrical ethers from n-alcohols, avoiding byproducts as olefins [23-26]. However, to
92 the best of our knowledge the synthesis of di-n-butyl ether does not have been reported on ion-
93 exchangers. Thus, the aim of the present paper is to study the liquid-phase dehydration of 1-
94 butanol to DNBE over t ion-exchange resins of different morphology and discuss the
95 relationship between resins properties and their catalytic behavior. Influence of typical 1-
96 butanol impurities on 1-butanol dehydration reaction is also discussed.

97 **2. Experimental**

98 **2.1. Chemicals**

99 1-butanol (≥ 99.4% pure; ≤ 0.1% butyl ether; ≤ 0.1% water) and 2-methyl-1-propanol (≥
100 99.45% pure; ≤ 0.05% water) supplied by Acros Organics, acetone (≥ 99.8% pure; ≤ 0.2%
101 water) supplied by Fisher Chemical and ethanol (≥ 99.8% pure; ≤ 0.02% water; ≤ 0.02%
102 methanol; ≤ 0.02% 2-Butanol) supplied by Panreac were used as reactants.
103 DNBE (≥ 99.0% pure; ≤ 0.05% water) supplied by Acros Organics, 1-butene (≥ 99.0% pure)
104 supplied by Sigma Aldrich, cis-2-butene (≥ 98.0% pure) supplied by TCI and water were used
105 for analysis purposes.

106 **2.2. Catalysts**

107 Tested catalysts were acidic styrene-codivinylbenzene ion exchange resins: the monosulfonated
108 macroreticular ones Amberlyst 15, Amberlyst 16 and Amberlyst 39 (high, medium and low
109 crosslinking degree, respectively); the oversulfonated macroreticular resins (in which the
110 concentration of $-HSO_3$ groups has been increased beyond the usual limit of one group per
111 benzene ring [27]) Amberlyst 35 (high crosslinking degree) and Amberlyst 36 (medium
112 crosslinking degree) which are oversulfonated versions of Amberlyst 15 and Amberlyst 16
113 respectively; the chlorinated macroreticular resins Amberlyst 70 and CT-482; the macroreticular
114 resin sulfonated exclusively at the polymer surface Amberlyst 46; and the monosulfonated gel-
115 type resins Dowex 50Wx8, Dowex 50Wx4, Amberlyst 31, Dowex 50Wx2 and Amberlyst 121
116 containing from 8 to 2 DVB%. Short names and properties are given in Table 1.

117 Table 1.

118 It is well known that ion-exchange resins swell in polar media. As a result, morphology changes
119 and non-permanent pores appear. Table 2 shows the morphological parameters both in dry state
120 and swollen in water of tested resins. As seen, macroreticular resins present BET surface areas
121 ranging between $0.02 - 57.4 \text{ m}^2/\text{g}$ (pore volume between $0.0 - 0.328 \text{ cm}^3/\text{g}$). Nevertheless, the
122 same resins show a surface area (and pore volume) increase up to $147 - 214 \text{ m}^2/\text{g}$ ($0.333 - 1.05$
123 cm^3/g) when swelling in water making clear that new pores with lower pore diameter appear. A
124 useful description of the nature and characteristics of these spaces can be obtained from Inverse
125 Steric Exclusion Chromatography (ISEC) data. In macroreticular resins a part of these new open
126 spaces in the range of mesopores can be characterized by the cylindrical pore model (“true
127 pores”). However, this model is not applicable to describe spaces between polymer chains in the
128 in the swollen polymer (micropores). A good view of the three-dimensional network of swollen
129 polymer is given by the geometrical model developed by Ogston [29] in which micropores are
130 described by spaces between randomly oriented rigid rods. The characteristic parameter of this
131 model is the specific volume of the swollen polymer (volume of the free space plus that
132 occupied by the skeleton), V_{sp} . The Ogston model also allows to distinguish zones of swollen
133 gel phase of different density or polymer chain concentration (total rod length per volume unit

134 of swollen polymer, nm^{-2}). According to Ogston model, density of polymer chains is described
135 as the total rod length per unit of volume. Figure 1 shows the distribution of different polymer
136 density zones of swollen catalysts in aqueous phase. As seen, gel-type resins Amberlyst 121,
137 Dowex 50Wx2, Amberlyst 31 and Dowex 50Wx4 and macroreticular resins with low
138 crosslinking degree Amberlyst 70 and Amberlyst 39 show low polymer densities ($0.2 - 0.8 \text{ nm}^{-2}$)
139 typical of an expanded polymer whereas macroreticular resins with medium and high
140 crosslinking degree CT-482, Amberlyst 36, Amberlyst 16, Amberlyst 35, Amberlyst 15 and
141 Amberlyst 46 present high chains concentration ($1.5 - 2 \text{ nm}^{-2}$) characteristic of a very dense
142 polymer mass. It is to be noted that Dowex50Wx8, in spite of being a gel-type resin, shows
143 zones with high polymer density (2 nm^{-2}). That behavior is probably due to its high DVB%.

144 Table 2.

145 Figure 1.

146 **2.3. Apparatus**

147 Experiments were carried out in a 100-mL-cylindrical high pressure autoclave made of 316
148 stainless steel (maximum temperature: $232 \text{ }^\circ\text{C}$; pressure range: $0 - 150 \text{ bar}$). It was equipped
149 with a magnetic drive stirrer and with a 400 W electrical furnace for heating. Temperature was
150 measured by a thermocouple located inside the reactor and stirring speed was measured by a
151 tachometer. Both operation variables were controlled to $\pm 1^\circ\text{C}$ and $\pm 1 \text{ rpm}$ respectively by an
152 electronic control unit. An injection system attached to the reactor was used to load the catalyst
153 once the operating conditions were reached. One of the outlets of the reactor was connected
154 directly to a liquid sampling valve, which injected $0.2 \text{ }\mu\text{L}$ of pressurized liquid into a gas-liquid
155 chromatograph.

156 **2.4. Analysis**

157 In order to follow the course of the reaction, the composition of the liquid mixture was analyzed
158 in-line by a 7820A GC System equipped with a TCD detector able to measure the presence of
159 water. The capillary column used was a dimethylpolysiloxane HP-Pona ($50 \text{ m} \times 0.200 \text{ mm} \times$

160 0.50 μm). Helium was used as the carrier gas ($70 \text{ mL}\cdot\text{min}^{-1}$, constant flow). Chromatograph
161 parameters were: volume injection $0.2 \mu\text{L}$; split ratio 100:1; injector temperature $150 \text{ }^\circ\text{C}$; oven
162 program: $45 \text{ }^\circ\text{C}$ for 5.5 min, $50 \text{ }^\circ\text{C}\cdot\text{min}^{-1}$ up to $180 \text{ }^\circ\text{C}$ which was held for 5 min. TCD
163 parameters were: detector temperature $250 \text{ }^\circ\text{C}$; reference flow $20 \text{ mL}\cdot\text{min}^{-1}$; makeup flow 4.9
164 $\text{mL}\cdot\text{min}^{-1}$.

165 A second GC equipped with a MS (Agilent GC/MS 5973) and chemical database software was
166 used to identify all the species.

167 **2.5. Methodology and calculations**

168 **2.5.1. Resin screening**

169 Wet resins (as provided by the supplier) were dried at room temperature during 24 h prior to
170 undergo mechanical sieving. Resin samples with bead size between $0.40 - 0.63 \text{ mm}$ were dried
171 at $110 \text{ }^\circ\text{C}$, firstly at 1 bar during 2 h and then at 10 mbar during 15 h. 1-butanol was charged in
172 the reactor and heated to $150 \text{ }^\circ\text{C}$. The reaction mixture was pressurized to 40 bar by means of N_2
173 in order to assure the liquid phase reaction medium. Stirring speed was set at 500 rpm. After
174 reaching the working temperature, 1 g of dry catalyst was injected by means of pneumatic
175 transport. That moment was considered the starting point of reaction. To follow the variation of
176 concentration of reactants and products with time, liquid samples were taken out hourly and
177 analyzed in-line as mentioned above. Total length of the experiments was 7 h. In all the
178 experiments mass balance was accomplished within $\pm 8\%$.

179 An additional series of experiments was performed over Amberlyst 31 and Amberlyst 15 to test
180 their thermal stability and reusability. These resins have one of the lower maximum operation
181 temperatures within the gel-type group and the macroporous group respectively (Table 1).
182 Each resin was used for three cycles. In the first cycle fresh catalysts were used following the
183 experimental procedure above mentioned. After a 7 h experiment the reactor was cooled at the
184 room temperature, catalyst was filtered out from the reaction medium, washed with 25 ml of

185 methanol, dried at ambient temperature during 24 h then dried at 110 °C, firstly at 1 bar during 2
 186 h and then at 10 mbar during 15 h before being subjected to a new reaction cycle.

187 In each experiment, 1-butanol conversion (X_{BuOH}), selectivity to products (S_j , the subscript j
 188 corresponding to each formed product) and DNBE yield (Y_{DNBE}) were estimated as follows:

$$X_{\text{BuOH}} = \frac{\text{mole of 1-butanol reacted}}{\text{initial mole of 1-butanol}} \quad (1)$$

$$S_{\text{DNBE}} = \frac{\text{mole of 1-butanol reacted to form DNBE}}{\text{mole of 1-butanol reacted}} \quad (2)$$

189 Selectivity to olefins ($S_{1\text{-butene}}$, $S_{(E)2\text{-butene}}$ and $S_{(Z)2\text{-butene}}$) branched ether 1-(1-methylpropoxy)
 190 butane (S_{BuOBu}) and 2-butanol ($S_{2\text{-BuOH}}$) were defined similarly.

$$Y_{\text{DNBE}} = \frac{\text{mole of 1-butanol reacted to form DNBE}}{\text{initial mole of 1-butanol}} = X_{\text{BuOH}} \cdot S_{\text{DNBE}} \quad (3)$$

191 In addition, initial reaction rate of DNBE formation (r_{DNBE}^0) was computed from the function of
 192 the experimental curve of DNBE mole (n_{DNBE}) vs. time according to:

$$r_{\text{DNBE}}^0 = \frac{1}{W_{\text{cat.}}} \left(\frac{dn_{\text{DNBE}}}{dt} \right)_{t=0} \quad (4)$$

193 Initial turnover frequency for DNBE formation ($\text{TOF}_{\text{DNBE}}^0$) was estimated by dividing r_{DNBE}^0 by
 194 the acid capacity:

$$\text{TOF}_{\text{DNBE}}^0 = \frac{r_{\text{DNBE}}^0}{\text{acid capacity}} \quad (5)$$

195 **2.5.2. Presence of byproducts in the feed composition**

196 The influence of typical 1-butanol impurities on the dehydration of 1-butanol to DNBE was
 197 studied. If 1-butanol is produced by the oxo process the main impurity is isobutanol whereas if
 198 it is produced by the ABE fermentation process impurities are and ethanol and acetone.
 199 Experiments were carried out with different mixtures of 1-butanol : isobutanol (95:5 and 90:10
 200 wt%) and 1-butanol:ethanol:acetone (95:2.5:2.5 and 90:5:5 wt%) over the highly selective

201 resins Amberlyst 70, Amberlyst 31 and Amberlyst 121. The experimental procedure and
202 reaction conditions were the same as for catalyst testing: 1g of dry catalyst, catalyst bead size
203 between 0.400 – 0.630 mm, 150 °C, 40 bar, 500 rpm, and 7 h.

204 3. Results and discussion

205 3.1. Reaction Network

206 Dehydration of 1-butanol over the ion exchange resins tested leads to the formation of di-n-
207 butyl ether as main product. Detected byproducts were C₄ olefins (1-butene, trans- and cis- 2-
208 butene), the branched ether 1-(1-methylpropoxy) butane and, in much smaller amount, 2-
209 butanol. Figure 2 shows the evolution of the liquid phase composition over the course of an
210 experiment conducted on Amberlyst 15. Products distribution on all tested resins is similar
211 although it should be pointed out some significant differences: (1) over macroreticular resins
212 with low crosslinking degree (Amberlyst 39 and Amberlyst 70) and gel type resins (Amberlyst
213 31, Amberlyst 121, Dowex 50x4 and Dowex 50x2) 2-butanol was not detected; (2) after 7 hours
214 reaction time most resins showed higher selectivity to 2-butenes than to 1-butene except for
215 Amberlyst 70, Amberlyst 121 and Dowex 50x2. This fact may be due to the very low total
216 amount of butenes formed on those resins.

217  Figure 2.

218 Distribution of products suggests the reaction network of Figure 3. Dehydration of 1-butanol to
219 di-n-butyl ether (DNBE) is the main reaction (R1). Dehydration to olefins is the main side
220 reaction (R2). The fact that at very low olefins concentration the major C₄ product was 1-butene
221 whereas when olefins concentration increase 2-butenes are favored, especially trans-2-butene,
222 indicates that 1-butanol dehydrates to 1-butene which in his turn isomerizes to trans-2-butene
223 and cis-2-butene (R3); the trans-isomer being thermodynamically more stable. The resins sites
224 are also active for catalyzing the reverse reactions of (R1) and (R2), ether hydrolysis (R4) and
225 olefin hydration (R5). When olefin hydration takes place, the alcohol that is formed is no longer
226 a primary alcohol. In addition to double bond isomerization, 2-butenes could be formed by
227 hydration of 1-butene to 2- butanol and its subsequent dehydration, giving place to any of the

228 three C₄ olefins. From the fact 1-(1-methylpropoxy)butane was detected over all the resins
229 despite the nonexistence of 2-butanol on some catalysts, it is inferred that the branched ether
230 could be preferably formed by 1-butanol reaction with a C₄ olefin (R6) instead of by the
231 reaction between 1-butanol and 2-butanol. Furthermore, the absence of 2,2'-oxydibutane
232 indicates that intermolecular dehydration of two molecules of 2-butanol is not taking place,
233 probably due to the low concentration of the secondary alcohol in the reaction medium.

234  Figure 3.

235 **3.2. 1-Butanol conversion, initial reaction rate, selectivity to DNBE and DNBE yield**

236 Table 3 shows 1-butanol conversion, selectivity to DNBE and byproducts, and yield of DNBE
237 at 7 h reaction time. Initial reaction rate and turnover frequency of DNBE synthesis are also
238 given. Data has a relative experimental error lower than $\pm 4\%$ for X_{BuOH} , $\pm 1\%$ for S_{DNBE} , $\pm 5\%$
239 for Y_{DNBE} and $\pm 7\%$ for r_{DNBE}^0 and $\text{TOF}_{\text{DNBE}}^0$. Due to the low concentration of byproducts in the
240 reaction medium, $S_{\text{byproducts}}$ data has in some cases a relative experimental error up to $\pm 20\%$.

241  Table 3.

242 Taking into account that some preliminary long-time experiments (>72 h) showed that
243 equilibrium conversions are higher than 85% at the working conditions, it is seen that at the end
244 of experiments the reaction medium is still far from equilibrium. From data of Table 3 it is seen
245 that the most active resins are the oversulfonated resins Amberlyst 36 and Amberlyst 35,
246 whereas the most selective ones are Amberlyst 121 > Dowex 50Wx2 > Amberlyst 70 >
247 Amberlyst 46 > Dowex 50Wx4 > Amberlyst 31. Resins Amberlyst 16 > Amberlyst 36 >
248 Amberlyst 15 > Amberlyst 35 show the lowest selectivity to ether.

249 By plotting the selectivity to DNBE as a function of X_{BuOH} (Figure 4) it is shown that, for all
250 tested resins, S_{DNBE} initially decreases and then stabilizes. As a consequence it can be concluded
251 that at these alcohol conversions, the differences observed in S_{DNBE} after 7 h of reaction time are
252 not due to the different reaction extent on each catalyst. On the contrary, they are a consequence
253 of the resins properties, in particular morphology and acid capacity

254

Figure 4.

255 Figure 5 show the response surfaces for conversion and selectivity as a function of acid capacity
256 and V_{sp} , which, together with polymer chain density, is a suitable way of characterizing the
257 polymeric structure of the resins gel type phase. As seen, acid capacity is the parameter which
258 plays the most important role regarding resins activity as it can be inferred from the almost
259 vertical arrangement of colors in the response surface of Figure 5(a). Nevertheless, selectivity to
260 DNBE is influenced by both acid capacity and resin structure as it can be drawn from the
261 diagonal arrangement of colors in the response surface of Figure 5(b).

262

Figure 5.

263 In order to elucidate the influence of acid capacity and polymer morphology on resins behavior,
264 obtained data have been arranged as shown in Figure 6. In this way it is easy to compare on one
265 side, the behavior of resins having the same acid capacity but different polymeric structure and,
266 on the other side, resins with similar values of swollen polymer volume but different acid
267 capacity. Data corresponding to Amberlyst 46 have been omitted in Figure 6 (a), (c) and (d) for
268 the sake of clarity.

269

Figure 6.

270 From Figure 6 it can be assumed that a higher acid capacity is essential to a more active catalyst
271 (Figure 6 (a) and (c)) but it also seems to affect the catalyst selectivity to DNBE in a negative
272 way (Figure 6 (b)). Regarding polymer morphology, it plays a decisive role on resin selectivity
273 to DNBE and, although not as significant as acid capacity, it also influences catalytic activity.
274 These facts can be observed by comparing resins with similar acid capacity but different pore
275 structure: (1) Amberlyst 35 and Amberlyst 36 (5.3 meq.H⁺/g), and (2) Amberlyst 15, Amberlyst
276 16, Amberlyst 39, Dowex 50Wx8, Amberlyst 31, Dowex 50Wx4, Amberlyst 121 and Dowex
277 50Wx2 (around 4.8 meq.H⁺/g). It can be seen that, as V_{sp} rises, S_{DNBE} progressively increases
278 until reaching an almost constant value of about 98 – 99% with gel-type resins containing $\leq 4\%$
279 DVB (Figure 6 (b)). However, in spite of the improvement in catalytic activity observed when

280 the V_{sp} increases from 0.823 cm³/g (Amberlyst 15) to 1.245 cm³/g (Amberlyst 16) a further
281 increase in V_{sp} leads to a slightly reduction of the resin activity (Figure 6 (a) and (c)).


282 It is a well-established fact that the alcohols dehydration reaction occurs mainly in the swollen
283 polymer mass [23]. Dehydration reaction to ether follows a S_N2 reaction mechanism in which 2
284 alcohol molecules are involved, whereas dehydration to olefins occurs by a monomolecular
285 reaction of elimination, E1 [30]. As Figure 1 shows, tested resins have zones of different
286 density or polymer chain concentration in the swollen polymer mass ranging from 0.1 to 2.0
287 nm/nm³. Very high polymer concentration (2 nm/nm³) entails a very dense polymer mass,
288 poorly accessible to 1-butanol which leads to a lower catalytic activity. Furthermore, in this
289 dense polymer zone the S_N2 reaction is limited to a great extent by steric hindrance and the
290 occurrence of the E1 reaction increases, hence giving place to lower S_{DNBE}. On the other hand,
291 low polymer concentration corresponding to a greatly expanded polymer enhances selectivity to
292 DNBE. However, too low polymer concentration gives place to a significant distance among its
293 active centers. In this case the probability of disposing the precise orientation of sulfonic groups
294 to form the reaction intermediate lessens and resins activity decreases. Thus, medium values of
295 polymer chain concentration may favor 1-butanol conversion. That could explain the behavior
296 observed in Figure 6 (a) and (c) where, among resins with acid capacity around 4.8 meq. H⁺/g,
297 Amberlyst 16 (V_{sp} = 1.245 cm³/g; polymer density = 0.8 – 1.5 nm/nm³) shows a 1-butanol
298 conversion and initial reaction rate higher than those determined on gel-type resins (which have
299 higher V_{sp} but polymer densities ranging between 0.2 – 0.8 nm/nm³). TOF⁰_{DNBE} data (Table 3)
300 confirm that resins with medium V_{sp} values shows higher reaction rates per catalytic site.

301 As for thermostable resins Amberlyst 70 and CT-482, the later has V_{sp} of 1.081 cm³/g (Table 2)
302 and acid capacity of 4.25 meq. H⁺/g (Table 1). This value of acid capacity is not very different
303 from 4.8 meq. H⁺/g and, as seen in Figure 6 (a) and (c), catalytic activity of resin CT-482 is in
304 agreement with data obtained for resins with 4.8 meq. H⁺/g. Amberlyst 70 shows smaller 1-
305 butanol conversion because of its low acid capacity (2.65 meq. H⁺/g, Table 2). Furthermore, it
306 can be seen that selectivity to the linear ether over Amberlyst 70, as well as over Amberlyst 46,

307 is equal to the maximum S_{DNBE} value found which corresponds to the gel-type resins Amberlyst
308 121 and Dowex 50Wx2. This high selectivity (and therefore, high DNBE content in the final
309 product) is extremely desirable from an environmental standpoint, in addition to the obvious
310 impact on capital requirements and operating costs.

311 As seen in Figure 6 (d) the highest DNBE yield is achieved on Amberlyst-36, nonetheless, gel-
312 type resins and Amberlyst-70 are more selective to the linear ether which makes them more
313 appropriate for industrial use. Among them, Amberlyst-70 can be considered as the most
314 suitable catalyst due to its thermal stability.

315 Finally, Figure 7 shows the combined effect of acid capacity and V_{sp} on S_{DNBE} for all tested
316 resins. As can be seen, S_{DNBE} correlates quite well with acid capacity/ V_{sp} ratio showing that
317 selectivity to DNBE increases as the number of acid sites per volume unit of swollen polymer
318 (acid density) decreases.

319  Figure 7.

320 3.3. Thermal stability and reusability tests

321 Thermal stability and reusability test were conducted over Amberlyst 15 and Amberlyst 31.
322 These two resins were selected because they have a maximum operating temperature very much
323 lower than 150°C. Afterwards, BET surface area and acid capacity were measured and
324 compared to those of fresh catalyst. As shown in Table 4 both resins experience some loss of
325 sulfonic acid groups after 3 cycles (fresh resin plus two reused cycles; 21 h of accumulated
326 working time). BET surface area increases moderately in the case of Amberlyst 15. Despite the
327 small morphological and acid capacity change, performance of the two resins keeps constant
328 throughout the 3 cycles, as it can be seen in **Error! No s'ha trobat l'origen de la referència.**,
329 pointing out that results are not influenced by thermal deactivation and resins can be reused a
330 few cycles. In order to take into account the differences in initial alcohol and catalysts mass
331 (due to small catalysts losses in recovering and cleaning the resin operations), the factor X_{1-}
332 $\text{BuOH} \cdot n_{1-\text{BuOH}}^0 / W_{\text{cat}}$ is used instead of $X_{1-\text{BuOH}}$. The differences observed for r_{DNBE}^0 between **Error!**
333 **No s'ha trobat l'origen de la referència.** data and values gathered in Table 2 for Amberlyst 31

334 and Amberlyst 15 are due to the fact that in this series of experiments the injector was not used.
335 Thus, catalyst was charged into the reactor and then heated to 150°C; the moment in which this
336 temperature was reached was considered as the beginning of the experiment (zero time). It is to
337 be noted that despite this change of methodology the results are quite similar. It is concluded
338 from these reusing experiments that data reported in Table 3 are reliable. It can be accepted that
339 accessible zone of resins increases on losing active centers, and this effects are mutually
340 balanced. However, as resins show a clear trend to morphological instability it is suitable to use
341 resins with high thermal stability such us Amberlyst 70 for industrial application.

342 Table 4.

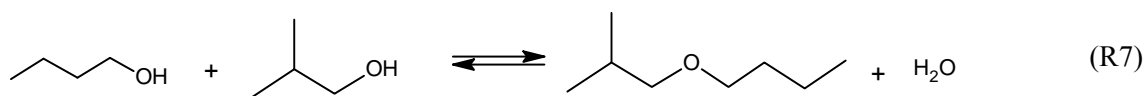
343 Figure 8.

344 **3.4. Influence of typical 1-butanol impurities**

345 **3.4.1 Influence of 2-methyl-1-propanol (isobutanol)**

346 Figure 9 shows the influence of isobutanol presence on the dehydration of 1-butanol to DNBE
347 at 7 h reaction. As seen, the trend is very similar over the three tested resins: the selectivity to
348 DNBE decreases on increasing the initial concentration of the branched alcohol mainly due to
349 the increment in 1-(1-methylpropoxy)butane formation. It is quoted in the open literature that
350 alcohols can undergo alkyl group transpositions [31]. In primary alcohols, after protonating to
351 form the alkyloxonium ion, steric hindrance interferes in the direct displacement of the leaving
352 group (water) by the nucleophile; instead water leaves at the same time as the alkyl group shifts
353 from the adjacent carbon to skip the formation of the unstable primary carbocation. This
354 mechanism is known as “Concerted Alkyl Shift” (Figure 10). Thus, the increasing amounts of
355 1-(1-methylpropoxy)butane detected when isobutanol is initially in the reaction medium is
356 explained by the reaction of 1-butanol with the secondary carbocation which results from
357 isobutanol dehydration and alkyl group shift. The rearrangement of products during isobutanol
358 dehydration in the presence of strong Brönsted acid sites is also reported by Kotsarenko and
359 Malysheva [32]. 1-(2methylpropoxy) butane was also detected in the reaction medium over the

360 three tested resins when isobutanol was added into the feed composition. This new branched
361 ether is formed when a molecule of isobutanol reacts with a molecule of 1-butanol (R7).



362 No significant change was observed on olefins concentration despite the addition of isobutanol
363 in the reaction medium. Olefin 2-methyl propene (isobutylene) consequence of isobutanol
364 intermolecular dehydration was not detected at these reaction conditions, probably due to the
365 low isobutanol initial concentration and conversion extent. However, even though the amount of
366 olefins, which are the most problematic byproduct, hardly changes by the isobutanol presence in
367 the initial reaction mixture, it should be avoided as it increases the formation of branched ethers
368 which present worse performance properties than the linear ether [8].

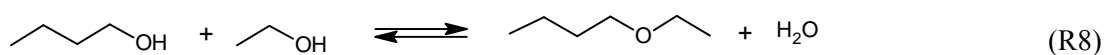
369 Figure 9.

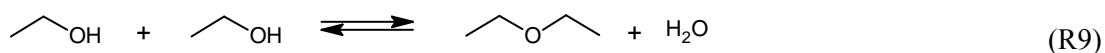
370 Figure 10.

371 3.4.2. Influence of ethanol and acetone

372 Two new byproducts were mainly detected when ethanol and acetone were added into the feed
373 composition: the major one was ethyl butyl ether (EBE) which is formed by the dehydration
374 reaction between a molecule of 1-butanol and a molecule of ethanol (R8); the another one,
375 detected only in very low amounts, was di-ethyl ether (DEE) which is the product of ethanol
376 intermolecular dehydration (R9).

377 As it can be seen in Figure 11 selectivity to DNBE decreased whereas EBE formation increased
378 when the initial amount of ethanol rises even at high 1-butanol:ethanol initial ratios. Similarly,
379 in the dehydration reaction of 1-octanol/ethanol mixtures at 150°C over acidic ion exchangers,
380 ethers with lower molecular weight are preferentially formed [33]. At present experimental
381 conditions the small amount of DEE detected is due to the high initial 1-butanol:ethanol ratios.
382 DEE must be avoided as it cannot be blended directly into commercial diesel fuels.





383 Regarding acetone reactivity, its condensation/dehydration forming mesityl oxide (MSO) and
 384 water over Amberlyst 16 in the temperature range 100 - 120 °C has been quoted [34]. Still,
 385 under the current experimental conditions acetone hardly react and only very low amounts of 2-
 386 propanol were detected (always less than 0.04% chromatographic area/g of catalyst). 2-Propanol
 387 could be the product of the acetone hydrogenation catalyzed by component of stainless steel
 388 tubing's and reactor walls such as nickel or iron. The amount of olefins (1-butene, trans-2-
 389 butene and cis-2-butene) and the branched ether 1-(1-methylpropoxy)butane did not experiment
 390 significant changes despite ethanol/acetone addition. Comparing the catalytic behavior of the
 391 three resins it can be concluded that, as found when isobutanol was added, the presence of
 392 ethanol and acetone in the reaction medium does not change significantly the general trend
 393 observed when 1-butanol is free of impurities.

394 Figure 11.

395 **4. Conclusions**

396 Sulfonic S/DVB resins are shown to be suitable catalysts for the dehydration reaction of 1-
 397 butanol to di-n-butyl ether in the liquid phase. Activity (reaction rate and conversion of 1-
 398 butanol) is enhanced with higher acid capacity (oversulfonated resins) and with medium values
 399 of swollen polymer volume (0.823 – 1.245 cm³/g). Very high polymer concentration entails a
 400 very dense polymer mass, poorly accessible to 1-butanol. On the contrary, very low polymer
 401 concentration corresponds to a greatly expanded polymer which gives place to a high distance
 402 among its active centers. As a result, the probability of disposing the precise conformation of
 403 sulfonic groups to form the reaction intermediate lessens and 1-butanol conversion decreases.
 404 Amberlyst 36 (oversulfonated, medium values of %DVB) has proved to be the most active
 405 catalysts tested. However, gel-type resins (which have a flexible morphology and are able to
 406 greatly swell in the reaction medium) and the resins Amberlyst-70 and Amberlyst-46 are more
 407 selective to DNBE; the resin Amberlyst 121 being the most selective. DNBE formation follows

408 a S_N2 reaction mechanism in which 2 molecules of 1-butanol are involved, whereas dehydration
409 to butenes occurs through a monomolecular reaction of elimination, E1. As a consequence, in
410 highly expanded polymers the S_N2 reaction is not limited by steric hindrance yielding higher
411 selectivity to the linear ether. In addition, a clear relationship between selectivity and H⁺/V_{sp}
412 ratio has been observed; the resins with lowest H⁺/V_{sp} being the most selective.

413 The presence of 2-methyl-1-propanol in the initial reactant mixture enhances the formation of
414 branched ethers, which have worse properties as diesel components than linear ones. However
415 no significant changes were observed in the concentration of olefins which are the most
416 troublesome byproducts regarding the sought properties for fuel additives. On the other hand,
417 the presence of ethanol and acetone leads to the formation of ethyl butyl ether and di-ethyl ether
418 but in a much lesser extent. Di-ethyl ether must be avoided as it cannot be blended directly into
419 commercial diesel fuels.

420 5. Acknowledgment

421 Financial support was provided by the Science and Education Ministry of Spain (project:
422 CTQ2010-16047). The authors thank Rohm and Haas France and Purolite for providing
423 Amberlyst and CT ion-exchange resins, respectively. We also thank Dr. Karel Jerabek of
424 Institute of Chemical process Fundamentals (Prague, Czech Republic) for the morphological
425 analyses made by the ISEC method

426 6. Nomenclature

AAS	amorphous aluminosilicate
ABE	acetone-butanol-ethanol
BET	Brunauer-Emmet-Teller
CFPP	cold filter plugging point
CP	cloud point
d _{pore}	mean pore diameter (nm)
EBE	ethyl butyl ether
DEE	di-ethyl ether
ISEC	inverse steric exclusion chromatography
DNBE	di-n-butyl ether
MSO	mesityl oxide
n _{DNBE}	mole number of di-n-butyl ether (mol)
RVP	Reid vapor pressure
r _{DNBE} ⁰	initial reaction rate (mol/h·kg of dry catalyst)

S_j	selectivity to product j
S_{area}	surface area determined from ISEC data (m^2/g)
S_{BET}	BET surface area (m^2/g)
S/DVB	styrene-divinylbenzene
t	time (h)
V_{pore}	pore volume (cm^3/g)
V_{sp}	volume of the swollen polymer (cm^3/g)
$W_{\text{cat.}}$	catalyst mass (dried) (g)
WHSV	weight hourly space velocity (h^{-1})
X_{BuOH}	conversion of 1-butanol
Y_{DNBE}	yield of di-n-butyl ether

Subscripts

BuOBu'	1-(1-methylpropoxy) butane
BuOH	1-butanol
2-BuOH	2-butanol

Greek letters

θ	porosity (%)
ρ_s	skeletal density (g/cm^3)

427 7. References

- [1] L.S. Ott, B. L. Smith, T. J. Bruno, *Energy Fuels* 22 (2008) 2518-2516.
- [2] M.N. Nabi, D. Kannan, J.E. Hustad, M.M. Rahman, in: *Role of Oxygenated Fuel to Reduce Diesel Emissions: A Review*. International Conference on Mechanical Engineering, Dhaka, Bangladesh, 2009.
- [3] A. Golubkov, *Motor Fuels for diesel engines*. Patent WO2001018154 A1 (2001).
- [4] T.J.A. Alander, A.P. Leskinen, T.M. Raunemaa, L. Rantanen, *Environ. Sci. Technol.* 38 (2004) 2707-2714.
- [5] A. Arteconi, A. Mazzarini, G. Di Nicola, *Water, Air, Soil, Pollut.* 221 (2011) 405-423.
- [6] I. Sezer, A. Bilgin, *Energy Fuels.* 22 (2008) 1341-1348.
- [7] R.L. McCormick, J.D. Ross, M.S. Graboski, *Environ. Sci. Technol.* 31 (4) (1997) 1144-1150.
- [8] G. C. Pecci, M.G. Clerici, F. Giavazzi, F. Ancillotti, M. Marchionna, R. Patrini, *IX International Symposium on Alcohol Fuels*, 1 (1991) 321-326.

- [9] M. Marchionna, R. Patrini, F. Giavazzi, G. C. Pecci, Symposium on Removal of Aromatics, Sulfur and Alkenes from Gasoline and Diesel, 212th National Meeting, ACS, (1996) 585-589.
- [10] L. S. Starkey, Introduction to Strategies for Organic Synthesis, Wiley, Hoboken, NJ, 2012. Chapter 3.3
- [11] R.A. Sheldon, H. van Bekkum, Fine Chemical through Heterogeneous Catalysis, Wiley-VCH, Weinheim (Germany), 2001, Chapter 6.5.
- [12] Chemsystems Perp Program, Oxo Alcohols PERP 06/07-08. www.chemsystem.com (07/2013)
- [13] T. Tsuchida, S. Sakuma, T. Takeguchi, W. Ueda, Ind. Eng. Chem. Res. 45 (2006) 8634-8642.
- [14] R. Cascone, Chem. Eng. Progress 104(8) (2008) S4-S9
- [15] <http://www.biofuelstp.eu/butanol.html> European Biofuels Technology Platform (07/2013)
- [16] Anonymous, Chem. Eng. Progress 103 (2007) 14.
- [17] R. J. J. Nel, A. de Klerk, Ind. Eng. Chem. Res. 48 (2009) 5230-5238.
- [18] M. A. Makarova, E. A. Paukshtis, J. M. Thomas, C. Williams, K. I. Zamaraev, J. Catal. 149 (1994) 36-51.
- [19] F.M. Bautista, B. Delmon, Appl. Catal. A: General. 130 (1995) 47-65.
- [20] P. Brandão, A. Philippou, J. Rocha, M. W. Anderson, Catal. Letters 80 (3-4) (2002) 99-102
- [21] J. H. Choi, J. K. Kim, D. R. Park, S. Park, J. Yi, I. K. Song, Catal. Commun. 14 (2011) 48-51.
- [22] J. K. Kim, J. H. Choi, J. H. Song, J. Yi, I. K. Song, Catal. Commun. 27 (2012) 5-8
- [23] J. Tejero, F. Cunill, M. Iborra, J.F. Izquierdo, C. Fité, J. Mol. Catal. A: Chem. 182 (2002) 541-554.

- [24] R. Bringué, M. Iborra, J. Tejero, J.F. Izquierdo, F. Cunill, C. Fité, V.F. Cruz, *J. Catal.* 244 (2006) 33-42.
- [25] E. Medina, R. Bringué, J. Tejero, M. Iborra, C. Fite, *Appl. Catal. A: General.* 374 (2010) 41-47.
- [26] C. Casas, R. Bringué, E. Ramírez, M. Iborra, J. Tejero, *Appl. Catal. A: General.* 396 (2011) 129-139.
- [27] K. Jerabek, L. Hantova, Z. Prokop, 12th International Congress on Catalysis, Granada (Spain), 2000.
- [28] S. Fisher, R. Kunin, *Anal. Chem.* 27 (1955) 1191-1194.
- [29] A.G. Ogston, *Trans. Faraday Soc.* 54 (1958) 1754-1757.
- [30] G.A. Olah, T. Shamma, G.K. Surya Prakash, *Catal. Lett.* 46 (1997) 1-4.
- [31] K.P.C. Vollhardt, N.E. Schore, *Química Orgánica*, 2nd Edition, Ed. Omega, Barcelona (Spain), 2000, Chapter 9.3.
- [32] S. Kotsarenko, L.V. Malysheva, *Kinet. Katal.* 24 (1983) 877-882.
- [33] J. Guilera, R. Bringué, E. Ramirez, M. Iborra, J. Tejero, *Ind.Eng.Chem.Res.* 51 (2012) 16525-16530.
- [34] E. du Toit, R. Schwarzer, W. Nicol, *Chem. Eng. Sci.* 59 (2004) 5545-5550.

Table 1. Properties of tested catalysts

Catalyst	Short name	Structure ^a	DVB%	Sulfonation Type ^b	Acidity ^c (meq.H ⁺ /g)	T _{max} ^d (°C)
Amberlyst-15	A-15	M	20	M	4.81	120
Amberlyst-35	A-35	M	20	O	5.32	150
Amberlyst-16	A-16	M	12	M	4.8	130
Amberlyst-36	A-36	M	12	O	5.4	150
CT-482	CT-482	M	Medium	M	4.25	190
Amberlyst-70	A-70	M	8	M	2.65	190
Amberlyst-39	A-39	M	8	M	5.0	130
Dowex 50Wx8	DOW-8	G	8	M	4.83	150
Amberlyst-31	A-31	G	4	M	4.8	130
Dowex 50Wx4	DOW-4	G	4	M	4.95	150
Amberlyst-121	A-121	G	2	M	4.8	130
Dowex 50Wx2	DOW-2	G	2	M	4.83	150
Amberlyst-46	A-46	M	High	S	0.87	120

^a Macroreticular structure (M) or gel-type structure (G)

^b Monosulfonated (M), oversulfonated (O) or sulfonated only at the polymer surface (S)

^c Titration against standard base following the procedure described by Fisher and Kunin [28].

^d Information supplied by manufacturer

Table 2. Morphology of tested catalyst in dry state and swollen in water

Catalyst	ρ_s^a (g/cm ³)	Dry state			Swollen in water (ISEC method)				
		S_{BET}^b (m ² /g)	V_{pore}^c (cm ³ /g)	d_{pore}^d (nm)	"True Pores"			Gel polymer	
					S_{ISEC}^e (m ² /g)	V_{ISEC}^f (cm ³ /g)	d_{pore}^d (nm)	V_{sp} (cm ³ /g)	θ_{Total}^g (%)
A-15	1.416	42.01	0.328	31.8	157	0.632	16.1	0.823	51.5
A-35	1.542	28.90	0.210	23.6	166	0.623	15.0	0.736	52.3
A-16	1.401	1.69	0.013	29.7	149	0.384	10.3	1.245	56.2
A-36	1.567	21.00	0.143	27.0	147	0.333	9.1	0.999	52.1
CT-482	1.538	8.7	0.06	26.8	214	1.051	18.5	1.081	69.5
A-70	1.520	0.02			176	0.355	8.1	1.15	56.3
A-39	1.417	0.09	2.9x10 ⁻⁴	17.6	181	0.36	7.9	1.451	61.0
DOW8	1.430	0.23						1.627	57.0
A-31	1.426	0.10	3.3x10 ⁻⁴	15.3				1.933	63.7
DOW4	1.426	0.01						1.92	63.5
A-121	1.428	0.02	3.5x10 ⁻⁴	32.9				3.263	78.5
DOW2	1.426	1.32						2.655	73.6
A-46	1.137	57.4	0.263	19.2	186	0.48	10.3	0.16	0.0

^a Skeletal density measured by Helium displacement

^b BET (Brunauer-Emmet-Teller) surface area

^c Pore volume determined by adsorption-desorption of N₂ at 77 K

^d Mean pore diameter. Assuming pore cylindrical model: $4V_{pore}/S_{BET}$ or $4V_{ISEC}/S_{ISEC}$

^e Surface area determined from ISEC data

^f Pore volume determined from ISEC data

^g Porosity estimated as $100V_g/(V_{pore}+(1/\rho_s))$ in dry state and as $100(V_{ISEC}+V_{sp}-(1/\rho_s))/(V_{ISEC}+V_{sp})$ in swollen state

Table 3. Conversion of 1-butanol, selectivity to DNBE and byproducts, yield to DNBE at 7 h reaction, initial reaction rate and turnover frequency for DNBE formation (1 g catalyst, catalyst bead size = 0.400 – 0.630 mm, T = 150°C, P = 40 bar).

Catalyst	X _{BuOH} %	S _{DNBE} %	S _{1-Butene} %	S _{(E)2-Butene} %	S _{(Z)2-Butene} %	S _{2-BuOH} %	S _{BuOBu} ^c %	Y _{DNBE} %	r _{DNBE} ⁰ mol/h kg	TOF _{DNBE} ⁰ mol/h eq H ⁺
A-15	18.4	81.7	1.27	4.89	2.74	0.890	8.56	15.0	15.6	3.25
A-35	22.2	74.8	1.38	6.35	3.46	1.33	12.7	16.6	22.9	4.30
A-16	19.9	92.9	0.753	1.65	0.994	0.343	3.33	18.5	17.2	3.59
A-36	23.2	86.4	0.934	3.30	1.87	0.725	6.76	20.1	28.1	5.20
CT-482	19.3	95.8	0.707	0.917	0.634	0.215	1.74	18.4	15.8	3.72
A-70	14.1	98.7	0.479	0.120	0.096	trace	0.595	14.0	10.3	3.90
A-39	19.4	97.1	0.613	0.559	0.407	0.0798	1.21	18.8	16.1	3.21
Dow-8	19.4	96.2	0.644	0.795	0.551	0.191	1.60	18.7	15.8	3.26
A-31	18.9	98.1	0.513	0.321	0.235	0.0431	0.759	18.5	14.5	3.02
Dow-4	18.6	98.4	0.481	0.265	0.215	trace	0.679	18.3	13.8	2.79
A-121	17.6	99.1	0.423	0.0118	trace	0	0.440	17.5	13.2	2.75
Dow-2	18.4	98.9	0.379	0.151	0.136	0	0.458	18.2	12.7	2.64
A-46	3.25	98.7	trace	trace	trace	0	1.32	3.21	1.64	1.88

Table 4. Acid capacity and BET surface area of fresh and reused catalysts after 3 reaction cycles (7 h, 150 °C, 40 bar)

Catalyst	Acid site loss ^a (%)			S _{BET} ^b (m ² /g)	
				Fresh	Reused
Amberlyst 15	11.6	±	3.3	42.01	43.7
Amberlyst 31	8.6	±	1.9	0.10	0.10

^a Titration against standard base following the procedure described by Fisher and Kunin [28].

^b BET (Brunauer-Emmet-Teller) surface area.

2 Figure Captions

3 Figure 1. ISEC pattern in water for used resins

7 Figure 2. Evolution of reaction medium composition with time (1g of Amberlyst-15, catalyst
8 bead size = 0.400 – 0.630 mm, T = 150°C, P = 40 bar, 500 rpm): (▲) 1-butanol; (●) water; (■)
9 DNBE; (★) 1-butene; (◆) trans-2-butene; (●) cis-2-butene; (▣) 1-(1-methylpropoxy)butane; (▶)
10 2-butanol.

8 Figure 3. Scheme of reaction network.

12 Figure 4. S_{DNBE} as a function of 1-butanol conversion (1 g catalyst, catalyst bead size = 0.400 –
13 0.630 mm, T = 150 °C, P = 40 bar, 500 rpm): (a) gel-type resins: (▲) A-121, (■) A-31, (Δ)
14 Dow-2, (□) Dow-4, (●) Dow-8; (b) macroreticular resins: (◆) A-70, (+) A-39, (●) CT-482, (□)
15 A-16, (Δ) A-15, (■) A-36, (▲) A-35.

15 Figure 5. Response surfaces for: (a) 1-butanol conversion; (b) selectivity to DNBE as a function
16 of V_{sp} and Acid Capacity. t = 7 h, 1 g catalyst, catalyst bead size = 0.400 – 0.630 mm, T = 150
17 °C, P = 40 bar, 500 rpm.

19 Figure 6. Influence of V_{sp} on: (a) 1-BuOH conversion; (b) selectivity to di-n-butyl ether; (c)
20 initial reaction rate for DNBE synthesis; (d) DNBE yield. t = 7 h, 1 g catalyst, catalyst bead
21 size = 0.400 - 0.630 mm, T = 150 °C, P = 40 bar, 500 rpm. (○) resins with 4.8 meq.H⁺/g; (◆)
22 resins with 5.3 meq.H⁺/g; (■) resins with other values of acid capacity.

22 Figure 7. Selectivity to di-n-butyl ether at t = 7 h (1 g catalyst, catalyst bead size = 0.400 –
23 0.630 mm, T = 150 °C, P = 40 bar, 500 rpm) as a function of H^+/V_{sp} : (○) resins with 4.8
24 meq.H⁺/g, (◆) resins with 5.3 meq.H⁺/g, (■) resins with other values of acid capacity.

25 Figure 8. Conversion of 1-butanol ($X_{BUOH} \cdot n_{BuOH}^0 / W_{cata}$) and selectivity to DNBE (S_{DNBE}) at 7 h
26 reaction and initial reaction rate for DNBE formation (1 g catalyst, catalyst bead size = 0.400 –
27 0.630 mm, T = 150°C, P = 40 bar). (■) Amberlyst 15; (□) Amberlyst 31.

28 Figure 9. Influence of 2-methyl propanol on the dehydration of 1-butanol to DNBE at 7 h
29 reaction. T = 150 °C, P = 40 bar, 500 rpm, 1 g catalyst, catalyst bead size = 0.400 - 0.630 mm: (
30 ■) DNBE; (▣) Olefins; (▢) 1-(1-methylpropoxy) butane; (■) 1-(2-methylpropoxy) butane.

29 Figure 10. Mechanism of Concerted Alkyl Shift.

33 Figure 11. Influence of ethanol and acetone on the dehydration of 1-butanol to DNBE at 7 h
34 reaction. T = 150 °C, P = 40 bar, 500 rpm, 1 g catalyst, catalyst bead size = 0.400 - 0.630 mm: (
35 ■) DNBE; (▣) Olefins; (▢) 1-(1-methylpropoxy) butane; (▣) Ethyl butyl ether; (■) Diethyl
36 ether.

33 **Table Caption**

34 Table 1. Properties of tested catalysts.

35 Table 2. Morphology of tested catalyst in dry state and swollen in water.

36 Table 3. Conversion of 1-butanol, selectivity to DNBE and side products, yield to DNBE at 7 h
37 reaction, initial reaction rate and turnover frequency for DNBE formation (1 g catalyst, catalyst
38 bead size = 0.400 – 0.630 mm, T = 150°C, P = 40 bar).

39 Table 4. Acid capacity and BET surface area of fresh and reused catalysts after 3 reaction
40 cycles. (7 h, 150 °C, 40 bar).